Ballistic-Missile Research with Athena

ROBERT F. FRIEDMAN* AND JACK REED†
Atlantic Research Corporation, Duarte, Calif.

Athena was conceived to reduce the cost of ballistic-missile experimentation and employs comparatively inexpensive solid-propellant rockets to simulate the flight dynamics of intercontinental ballistic missiles. It is a four-stage, partially guided vehicle that has been launched from a point near Green River in south-eastern Utah and impacted at the White Sands Missile Range (WSMR) 420 naut miles away. The vehicle propels a variety of payloads into the atmosphere at various velocities and re-entry angles from altitudes ≤400,000 ft. The nominal performance requirements are 1) 50-lb payload delivered at 250,000 ft, 2) separation distances (fourth stage from payload) of at least 5000 ft at test altitudes, 3) velocity at test altitudes of 22,000 fps, 4) re-entry angles of 18° to 46°, and 5) payload angle of attack as close to zero as possible.

Nomenclature

$a.c.$	=	aerodynamic center
C_D	=	drag coefficient
$C_{N\alpha}$	=	normal-force slope coefficient
F_A	=	pitch frequency
h	=	altitude
M	=	Mach number
P	=	spin rate
R	=	range
S_{ref}	=	reference area
t	=	time
V_E	=	re-entry velocity
α	=	angle of attack
γ	=	flight path angle

Introduction

THE purpose of Athena is to place a payload at a designated point in space and at certain specified conditions so that useful re-entry experiments may be performed. The vehicle utilizes a simple ballistic trajectory and a programed re-entry angle capability of 18°–46°. For low-angle re-entry, it is reoriented by an 8°–10° yaw maneuver prior to third-stage ignition, such that the heading at re-entry is toward the Rampart site of the White Sands Missile Range. The nominal payload weight of 50 lb includes the actual payload and the ejection mechanism, which attaches to the payload interface structure. The payload is separated from the expended fourth stage before it reaches the test altitude of 250,000 ft in order to insure that it is clear of vehicle components that could interfere with the test objectives; testing is then conducted to impact. At 250,000 ft, $V_E \geq 22{,}000$ fps, and $\alpha \leq 5°$. A typical flight sequence is shown in Fig. 1.

The vehicle consists of four primary propulsion units, associated airframe, interstage structures, separation devices, spin and despin subsystems, telemetry subsystems, attitude-controller subsystems, and the remaining electronic and electrical installations. Functionally, the vehicle consists of two major sections: the booster and the velocity package. The booster package consists of the first two stages and associated aerodynamic fins; the velocity package consists of the upper two stages, a heat shield, an attitude controller, telemetry, and the experimental payload. The first two stages boost the velocity package to apogee. Reorientation and re-entry will be accomplished by the latter two stages. Light metal castings have been used on the booster stages wherever possible because of their relatively low cost, simplicity, and structural integrity. Since the aerodynamic and thermodynamic support structure for the velocity package will be discarded with the second stage, it is considered as part of the booster package.

Presented as Preprint 64-275 at the 1st AIAA Annual Meeting, Washington, D.C., June 29–July 2, 1964; revision received January 26, 1965.

* Project Engineer, Advanced Systems; now with the Douglas Aircraft Company, Inc., Advanced Systems and Technology, Santa Monica, Calif. Member AIAA.

† Program Manager, Athena Program.

Vehicle Design

The design of the Athena vehicle was predicted on the concept of booster vs velocity package combinations for meeting performance requirements. This concept provides reliable and economical booster hardware and permits the application of strength-to-weight optimization for high mass fraction velocity package stages. The resulting weight breakdown is given in Table 1.

To achieve the previously stated mission objectives, two Athena vehicles, Mod I and Mod II, were selected which differ only in the second-stage propulsion systems. The propulsion system selected insures high reliability, because the motors have been tested extensively in flight (Table 2). Mod I will provide re-entry angles from 18° to 30°; Mod II will provide re-entry angles from 40 to 46°. Other re-entry angles will require booster modifications. The over-all vehicle configuration (Fig. 2) and the selected rocket motors should be capable of meeting or exceeding the performance requirements with good reliability.

First Stage

A Thiokol (XM-33-E8) Castor motor and two Thiokol (XM-19-E1) Recruit motors comprise the first-stage propulsion system (Fig. 3). The Recruits, used to increase the

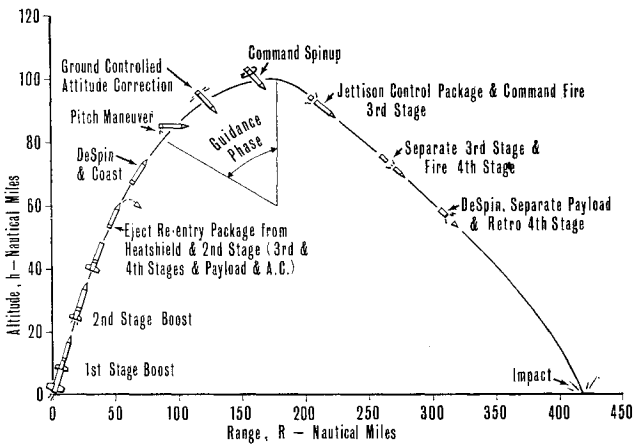

Fig. 1 Athena flight sequence.

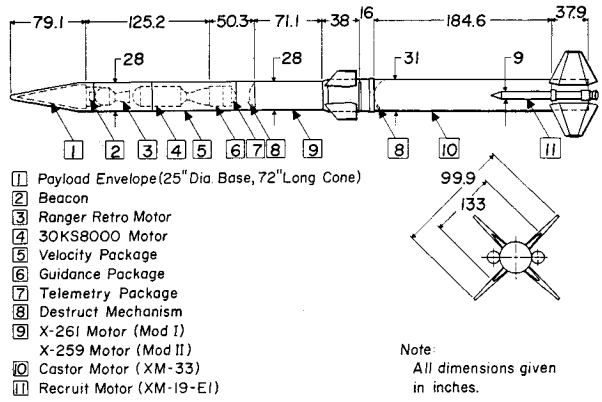

Fig. 2 Athena vehicle configuration.

longitudinal acceleration at launch, will burn out at approximately 1.9 sec after launch; their nozzles are canted to direct the thrust axis through the center of gravity of the launch vehicle, eliminating undesired motions if one Recruit fails to ignite. The Castor motor will be ignited by ground power at zero time; Recruit ignition will be delayed until a positive indication of Castor motion is sensed.

Spin rockets and the four canted first- and second-stage fins will produce a maximum spin rate of 3 rps after the vehicle leaves the launcher, minimizing dispersion due to body-attached disturbing influences. The fins also provide aerodynamic stability. Fin sizes for minimum vehicle dispersions (12 and 6 ft²/panel on the first and second stages, respectively) were determined from results of wind-tunnel experimentation[1, 2] and studies to determine the tradeoffs between aerodynamic stability, impact dispersion, and rail launcher lengths. The rail launcher has been used to reduce the effects of winds.

A command-destruct component is located on the forward section of the Castor motor. Should it be necessary to destroy the boost vehicle during the first stage of flight, a ground signal will be transmitted to a command receiver located in the after part of the velocity package assembly.

Second Stage

The first and second stages are joined by an adapter and separation assembly consisting of two double Marman clamps and two explosive nuts. The separation system is designed such that operation failure of one nut will not prevent first-stage separation. The Marman clamp system has been successfully operated in a variety of configurations where low-force separation was required. The second-stage motor (Fig.

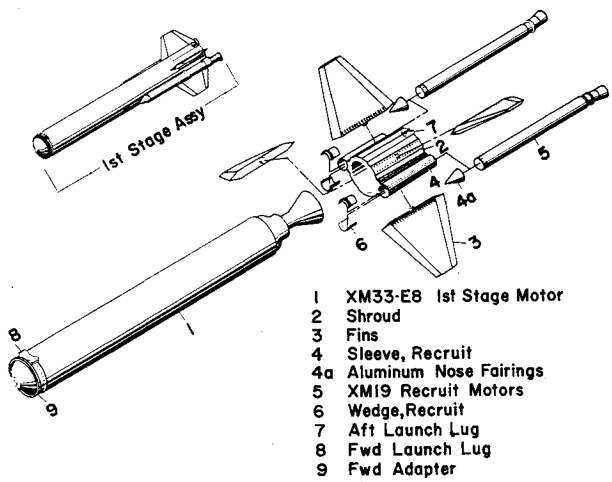

Fig. 3 First-stage assembly.

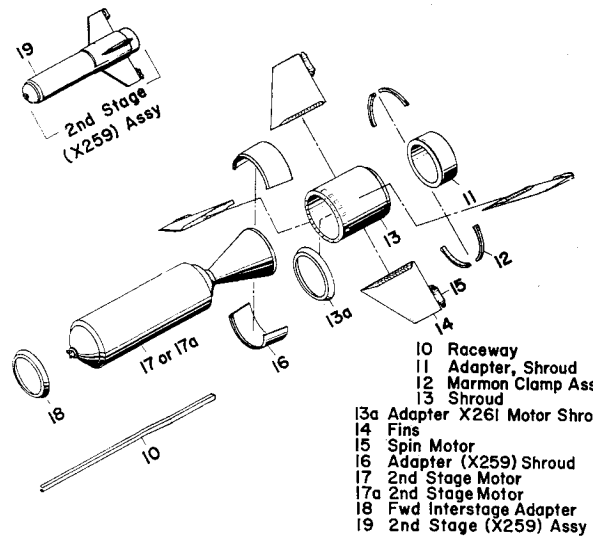

Fig. 4 Second-stage assembly.

4) used depends on the re-entry angle required for the payload test; for $\gamma_E = 18°$ to 30°, a Thiokol TX-261-2 motor is used (Mod I); for $\gamma_E = 40°$ to 46°, an Antares II X259A2 motor is used (Mod II). Because of the difference in motor diameters, the second-stage adapter assembly differs. A command-destruct system, located on the forward part of the motor, permits vehicle destruction during the second stage of flight. The four spin rockets that are ignited at launch are located on the trailing edges of the second-stage fins.

Velocity Package

The velocity package (Figs. 5 and 6) consists of the third- and fourth-stage motors, the guidance and control assembly, the spin and despin system, a retromotor, and a heat shield. The adapter assembly between the second stage and the velocity package contains a separation mechanism that is comprised of an air-spring bellows arrangement that expands by firing an explosive nut that releases the Marman clamp. The bellows will be pressurized between 50 and 70 psia at separation, and its travel will be limited to 7 in. by stop bolts. This mechanism will impart a ΔV of 12 fps to the velocity package. Two timers (one is redundant) within the adapter assembly (immediately behind the bellows) will initiate 1) first-stage separation, 2) second-stage motor ignition, 3) nose-cone removal, and 4) second-stage separation. A C-band radar beacon is provided to satisfy WSMR range safety and tracking requirements.

Third stage

The third stage comprises a guidance and control assembly and a third-stage motor assembly. The former contains the third-stage telemetry system, command receiver, and attitude control system. The motor assembly contains a

Table 1 Weight statement

Sequence	Weight, lb
4th-stage burnout	175
4th-stage ignition	368
3rd-stage burnout	535.5
3rd-stage ignition	1,416.1
Velocity package	1,645
2nd-stage burnout	3,297
2nd-stage ignition	5,630
1st-stage burnout	8,067.8
Recruit burnout	14,969.8
Launch	16,060.4

30KS8000 motor and yo-yo despin and spin-up motor systems. The PAM/FM/FM telemetry system is located inside the third-stage support tube behind the attitude controller and command receiver. It transmits on a frequency of 245.3 mc and has 17 continuous and one commutated Interrange Instrumentation Group (IRIG) standard subcarriers. Its function is to provide vehicle attitude and rate information (real time) data for the command link. It uses four quarter-wave, slotted-fin, circularly polarized antennas (mounted on the heat shield), which are coaxially switched to four quarter-wave, slotted-fin, circularly polarized antennas mounted on the support tube at the time of velocity package ejection. A similar telemetry system utilizing a frequency of 259.7 mc is used on the fourth stage for experimental flights.

The command receiver provides the signal to destruct the first and second stages independently and initiates a sequence of events prior to third-stage ignition. Since no destruct capability exists in the velocity package, the command to fire the third stage is not initiated unless a safe path has been indicated by the telemetry data. Once a safe path is confirmed, a signal from the ground initiates a mechanical timer that directs the following events: 1) ettisoning of the third-stage telemetry system, command receiver, attitude control system, and guidance and control assembly; 2) third-stage ignition; 3) third-stage separation; 4) ignition; and 5) despin of the expended fourth-stage plus payload and arming of the fourth-stage assembly accelerometers.

The attitude reference system consists of 2 two-degree-of-freedom gyros to sense displacement for pitch, yaw, and roll. Gyro errors are fed through associated control networks to activate six cold-nitrogen-gas reaction jets that orient the velocity package for re-entry. At launch, the gyros will be referenced to the nominal pointing vector. Although gyro reference is maintained during the first two stages of boost, the system is passive from a control sense. The timer of the attitude control system is initiated by a switch that is opened by the separation of the velocity package. The control system is not activated until after the velocity package has been despun by a yo-yo system mounted on the aft end of the adapter to the fourth stage. The yo-yo consists of two metal tapes with weights at their ends. It is initiated by a pyrotechnic pin-pulling device and timer, which are activated at velociy package separation.

After telemetry circuits determine that the velocity package has responded to final attitude control commands from the ground, two spin rockets, mounted on the circumference of the third-stage motor, respin the velocity package in order to limit the coning magnitude during third- and fourth-stage burning to a level commensurate with over-all angle of attack requirements. The spin motors are activated by a signal transmitted from the ground and received in the third-stage command receiver.

Fourth stage

The fourth-stage assembly (Fig. 6) consists of a payload support assembly that houses the Hercules BE-3-A4 fourth-stage motor, a chemical despin-respin system, a payload support structure, instrumentation, and retrorockets. The chemical despin-respin system consists of three despin and three respin rocket motors mounted on the motor circumference near the forward station of the BE-3-A4 motor.

Table 2 Past motor performance

Flight sequence	Motor	No. of flight tests	Failures
First stage	XM-33-E8	158	None
First-stage augmenters	XM-19E1	300	None
Second stage:			
Mod I	X-261	15	Mone
Mod II	X-259	17	None
Third stage	30KS8000	23	None
Fourth stage	BE-3	23	None

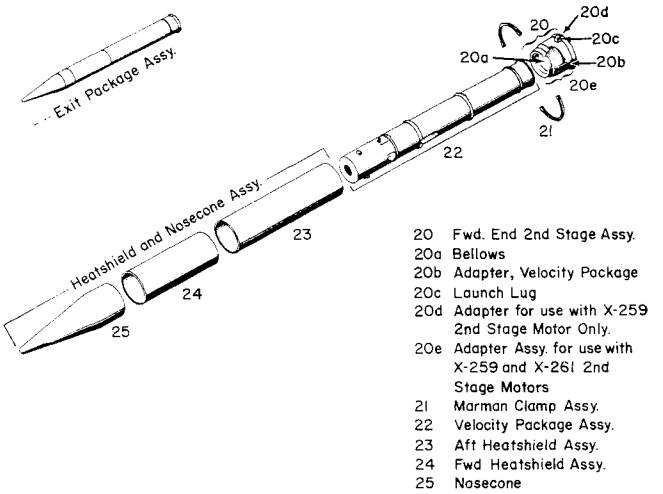

Fig. 5 Velocity package exit assembly.

The fourth stage is required to release the payload at a spin rate between 5 and 0.5 rps. The chemical despin-respin system (a 1 KS40 despin motor and a 1 KS40 respin motor) is used on this stage because a yo-yo system might confuse the radar or optical returns from the payload.

The instrumentation housing includes a *C*-band beacon (Fig. 2) for satisfying WSRM range safety and tracking requirements, and timers, batteries, and circuitry for ignition of the third- and fourth-stage motors, for initiation of fourth-stage despin-respin maneuvers, initiation of payload separation, and for ignition of four retrorockets which decrease acceleration of the expended fourth stage. Each retromotor exhaust nozzle is canted outboard of the longitudinal axis, assisting in avoidance of particle impingement of the separated payload.

Flight Operation

The flight-event sequence (Fig. 1) is summarized as follows. The vehicle is launched from a 30-ft rail launcher at nominal elevation angles of 75° and 76° and azimuth angles of 156° and 151° for Mod I and Mod II configurations, respectively. Figure 7 depicts the first, second, third, and fourth stage and payload impact areas. At first motion the Recruit motors

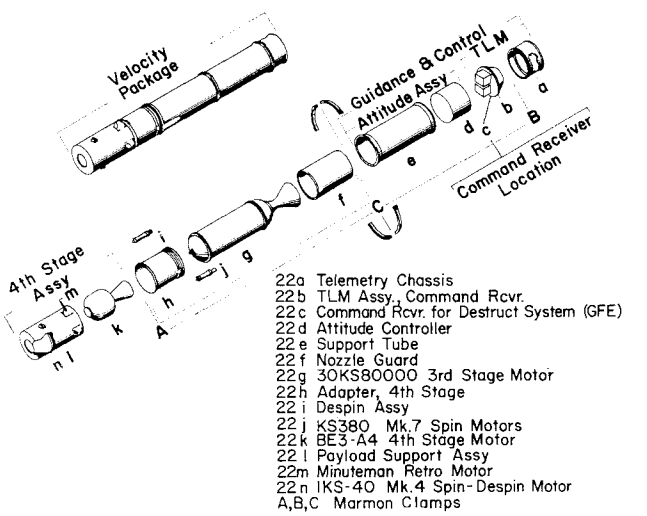

Fig. 6 Velocity package assembly.

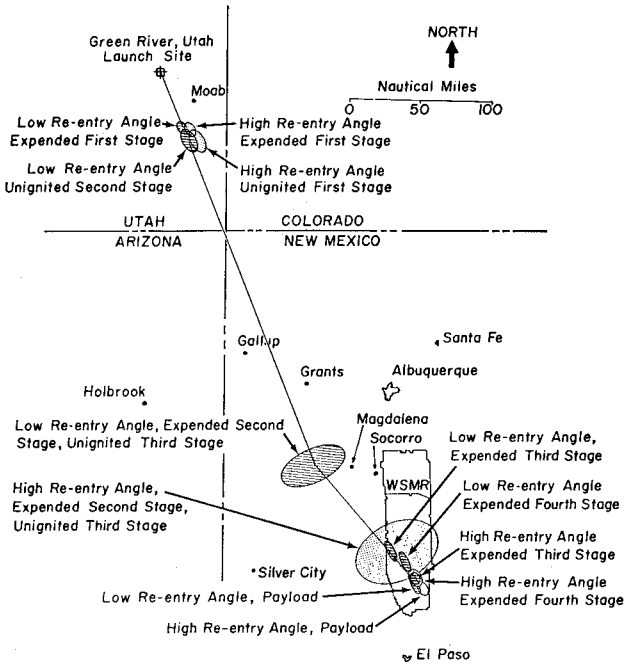

Fig. 7 Impact areas of the expended stages of the Athena and payload.

ignite. As the vehicle clears the launcher, the four spin motors mounted on the second-stage fins ignite, and spin is maintained during first- and second-stage operation by canted first- and second-stage fins in order to 1) average out thrust misalignments, thereby decreasing dispersions, and 2) provide stability for the vehicle at or near second-stage burnout altitudes. After ~40 sec, the first-stage motor burns out, the Marman clamp is released, and separation is achieved by normal drag build-up on the first stage. After a coast period, determined by the specific mission requirements, the second-stage motor is ignited. The second stage for Mod I (X-261-2 motor) burns ~13 sec, for Mod II (X-259 motor), ~34 sec. At 300,000 ft, the nose-cone heat shield is ejected by a set of peripherial springs, and the velocity package is ejected (ΔV ~12 fps) from the open front end of the cylindrical heat shield by the Marman-clamp-retained bellows at the forward end of the second-stage assembly. A spin rate of 3 rps is maintained as the velocity package ejects from the heat shield.

The velocity package is despun by a yo-yo mechanism, and simultaneous activation of the attitude controller removes all residual roll, pitch, and yaw. The ground-commanded attitude controller orients the velocity package to the approximate nominal re-entry attitude. During this maneuver and the subsequent coast period prior to third-stage ignition, ground tracking provides position and velocity in "real time" and predicts impact coordinates. Both telemetry guidance signals and the radar tracking information are analyzed by high-speed computers evaluating the accuracy of the velocity package response to the attitude-control commands. At this time, a signal is transmitted to the command receiver to respin the vehicle to a nominal 5 rps, and the attitude-controller gas jets are deactivated. If the spin rate, body motions, impact predictions, and telemetry and attitude-controller functions are acceptable, an additional signal is transmitted to activate a mechanical timer, which directs the following sequence of events: 1) jettison of guidance package, 2) third-stage motor ignition, 3) third-stage separation (release of a Marman clamp), 4) fourth-stage motor ignition, and 5) despin of expended fourth stage.

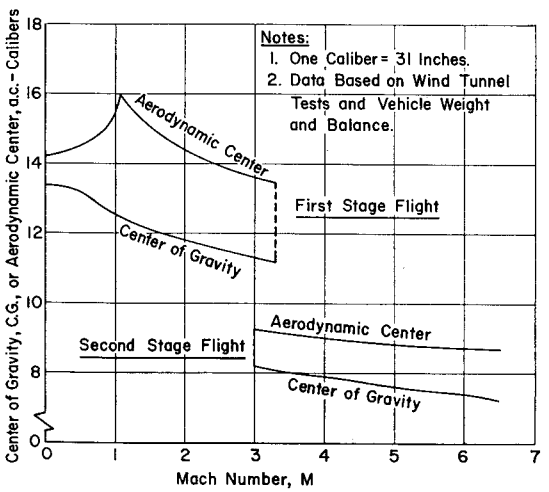

Fig. 8 Athena aerodynamic stability.

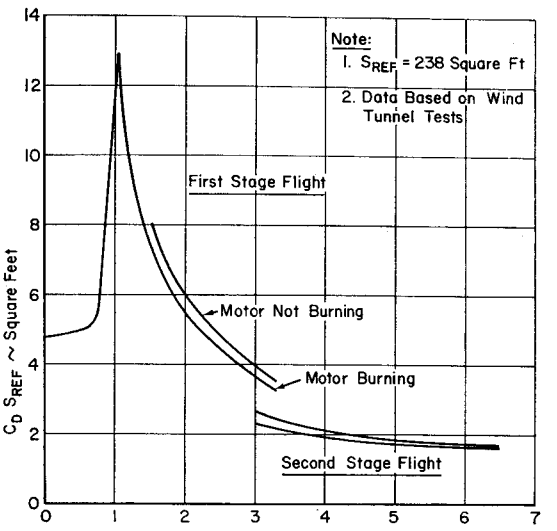

Fig. 9 Drag coefficients.

At a predetermined despin rate of the fourth stage, the respin motors are ignited. As the thrusts of the despin and respin motors become equal, no net change in rotational momentum occurs. At this time, the payload is separated with $\Delta V \simeq 10$ fps, and a spin rate will be between 1 and 2 rps, depending on the specification of the payload. Retromotors on the expended fourth stage slow it to assure a good separation from the payload.

Performance

The Athena system may be utilized for payloads in excess of 50 lb and/or test altitudes exceeding 250,000 ft. Payloads of more than 50 lb will decrease V_E at 250,000 ft, or, correspondingly, test altitudes in excess of 250,000 ft will result in lower V_E because of loss of the gravitational component of velocity. More important, however, less time is available for a "clean" separation distance between the expended fourth stage and the payload when payload altitudes exceed 250,000 ft.

Table 3 Payload sensitivity

Gross payload	Sensitivity factor ft/sec/lb
0–50	55
50–100	35
100–150	25
150–200	20
200–250	12

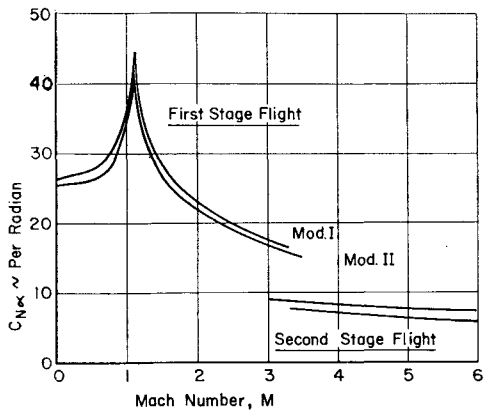

Note:
1. S_{REF} = 238 Square Feet
2. Data Based on Wind Tunnel Tests

Fig. 10 Normal force coefficients.

Aerodynamic and Dynamic Characteristics

During atmospheric flight, the vehicle is fin-stabilized; outside the normal atmosphere, it is spin-stabilized. Figure 8 contains data for aerodynamic center and center-of-gravity variation with Mach number for typical trajectories. Graphs of drag coefficients and normal-force slope coefficients are presented in Figs. 9 and 10. These aerodynamic data have been substantiated by wind-tunnel tests.[1, 2]

Vehicle spin rates about the longitudinal body axis as a function of flight time are shown in Fig. 11. The spin rates have been chosen to minimize the impact dispersions, to provide adequate spin stabilization outside the atmosphere, and to prevent pitch-roll coupling. No appreciable α is built up through coupling during the flight trajectory. For third- and fourth-stage burning, spin rates up to a maximum of 10 rps are obtainable. Prior to payload ejection, the vehicle system has the capability of reducing the spin rate to a predetermined value.

Re-Entry Performance

Achievable re-entry conditions for Mod I and Mod II are presented in Figs. 12 and 13. Data for these plots were obtained from a digital computer search routine that agrees with the six-degree-of-freedom program[3] used to establish the final trajectories. Two test altitudes were selected, 250,000 ft and 300,000 ft. The plots present payload re-entry velocity as a function of re-entry angle for gross payload weights ranging from 0 to 250 lb. Each plot depicts the second-stage impact limitation. The second-stage ballast weight and gross payload weights are variables.

Jet pluming effects[4] indicate that second-stage burnout altitudes should not exceed 192,000 ft for Mod I, because a precession half-angle greater than 5° would be created, which would degrade guidance system performance.

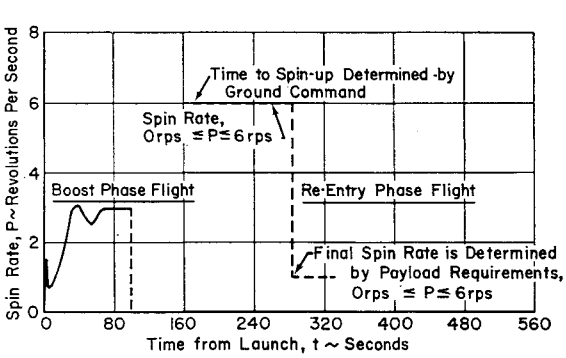

Fig. 11 Spin rates.

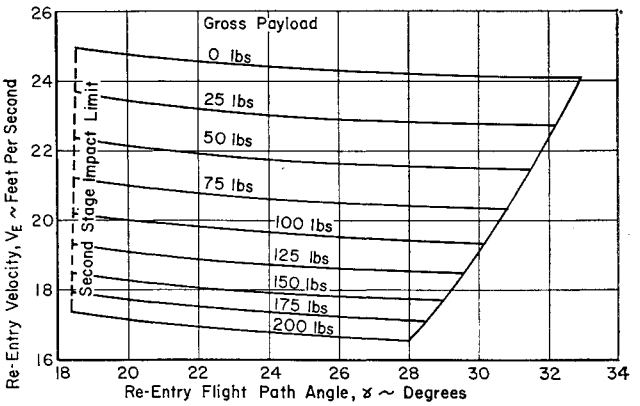

Notes: 1. Payload Test Altitude = 250,000 & 300,000 Feet.
2. Second Stage Impact 307 N.M. (Low Angle Re-Entry)
3. Time from 4th Stage Burnout to Payload Test Altitude = 15 Sec
4. Gross Payload is Weight in Excess of 4th Stage Ignition Weight of 288.4 Pounds.

Fig. 12 Athena Mod I re-entry performance.

All trajectories were based on a second-stage impact range of 307 naut miles for Mod I (low angle requirements) and 388 naut miles for Mod II (high angle requirements). Additional conditions of a maneuvering time (after second-stage burnout) greater than 100 sec and a time between fourth-stage burnout and the test altitude of at least 15 sec are imposed. The payload impact points for these trajectories are consistent with the Rampart look-angle requirements and the 2σ payload-dispersion areas.[5]

The basic weights associated with the performance data (Table 1) were established from structural criteria on flight loads and static environments. The re-entry performance evaluation indicates a need for second-stage ballast within the jet pluming boundaries. It is also evident that V_E is relatively insensitive to second-stage ballast weight, but is quite sensitive to the gross payload weight (Table 3).

Vehicle Trajectory Data

Computed trajectory data for a typical flight are presented in Fig. 14. These computed curves include all physical effects that will significantly influence the trajectory. The flight simulation was based on a six-degree-of-freedom flight path program.[3]

Impact Dispersion

An impact dispersion analysis system was conducted to determine the system tolerances and uncertainties that are

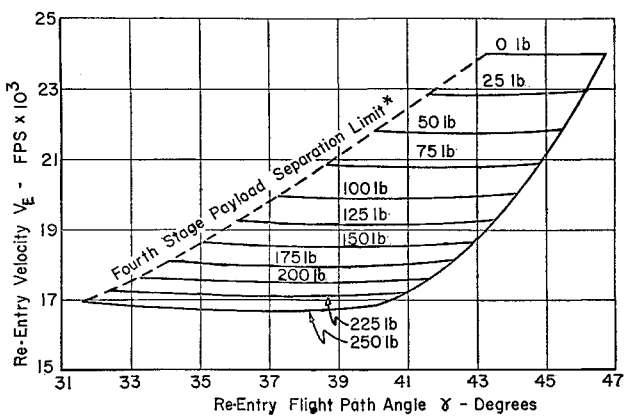

Notes: 1. Payload Test Altitude = 250,000 Ft
2. 2nd Stage Impact = 388 Mi. (High Re-Entry Angle)
*3. Time From 4th Stage Burnout to Payload Test Altitude = 15 Sec
4. Gross Payload is Weight in Excess of 4th Stage Ignition Weight of 288.4 Pounds

Fig. 13 Athena Mod II re-entry performance.

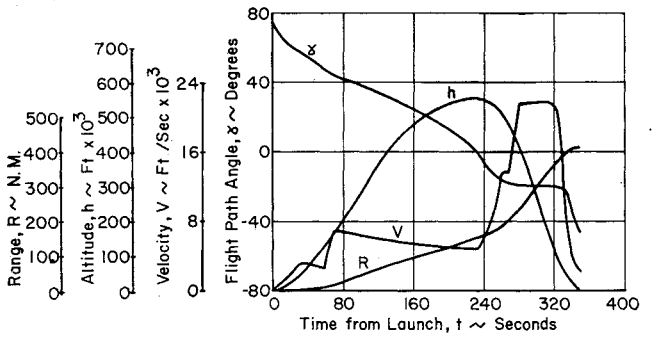

Notes: 1. Payload Weight = 50 lb
2. Second Stage Motor - X-261
3. Launch Angle, γ_L = 75 Degrees
4. Re-Entry Angle, γ_E = -20 Degrees
5. Re-Entry Velocity, V_E = 21,800 Ft /Sec.

Fig. 14 Typical flight trajectory for Athena.

commensurate with the 2σ impact dispersions illustrated in Fig. 7. The factors that contribute to the dispersion are 1) first-stage thrust misalignment, 2) wind-correction errors during ascent, 3) uncertainties in vehicle drag, 4) motor-propellant variations, 5) uncertainties in launcher settings, and 6) launcher rail tipoff.

Manufacturing tolerances may produce a misalignment of the thrust vector. Significant items considered were motor-center-of-gravity uncertainties and offset and misalignment tolerances of the interconnecting hardware. Inaccuracies in the meteorological system will cause uncertainties in wind profiles assumed for each launch condition. The error sources considered were the computational errors in launcher corrections for wind, the error caused by probable wind field changes between last wind measurement and vehicle launch, the errors in the wind measurement system, and the effect of vehicle aerodynamic and mass characteristic uncertainties on the vehicle wind response. Uncertainties in drag were established by uncertainties in the wind-tunnel data and in vehicle mass (the latter being determined from manufacturing tolerances and specifications for each motor). An analysis was conducted on the Athena launcher to determine the accuracy of launcher setting. Tipoff effects were determined from the dynamics of the rail as it affects the vehicle during launch.

Error sources that have a negligible effect of impact and have been omitted from the dispersion analysis are as follows: 1) first-stage fin alignment, 2) second-stage thrust and fin misalignment, 3) second-stage drag-coefficient variation, 4) second-stage ignition-time variation, 5) stage-to-stage misalignment, and 6) variations in vehicle mass characteristics and aerodynamic characteristics other than drag.

The effects of the following factors were considered (or assumed) in determining the 2σ errors:

1) The vehicle is launched from a 30-ft rail launcher to minimize dispersion from wind effects.

2) An analysis was conducted to determine the optimum vehicle spin rate. Factors taken into consideration were pitch-roll coupling, structural bending frequency, thrust misalignment effects, and fin misalignment effects. The effects on all stages are based on a controlled spin rate.

3) The effect of the combined errors is assumed to equal the root-sum-square (RSS) of the effects of the individual errors; i.e., total error = $[(\text{error}\,\#1)^2 + (\text{error}\,\#2)^2 + \ldots]^{1/2}$. This method produces the same number of standard deviations for the combined errors as is used for the individual errors. Each of the errors is statistically independent, occurring in a random manner with a nominal frequency distribution having a mean of zero.

4) Thrust misalignment, launcher pointing errors, wind and rail tipoff displace the impact in any direction, but drag uncertainty and motor performance variation will displace the impact in range only.

5) The influence of perturbations on the second stage has been established as the RSS of perturbations induced during first- and second-stage flight; this can be extended to N number of stages.

6) Effects of errors in wind drift on expended stages and pieces are not included because of their negligible effect on impact.

Conclusions

The Athena re-entry test vehicle can meet the test objectives of giving a nominal 50-lb re-entry payload a V_E on the order of 22,000 fps at 250,000 ft. Athena Mod I provides for γ_E = 18° to 30°, and Mod II provides γ_E + 40° to 46°. A high-mass-fraction velocity package is achieved by ejecting all of the thermodynamic and aerodynamic coverings prior to third-stage ignition and ejecting the guidance package once a safe orientation is established. The propulsion system selected insures a high degree of reliability in motor performance, because the motors have been tested extensively in flight. The ranges of V_E and γ_E could be extended by various combinations of second-stage motor configurations, ballast weights, and ignition time delays.

References

[1] "Supersonic wind tunnel test of Athena vehicle," unpublished data NASA Langley Research Center, Unitary Plan, Supersonic Wind Tunnel, Langley, Va. (1962).

[2] "Additional low speed, wind tunnel test of a $\frac{1}{2}$ scale model of ARC vehicle B, special test vehicle program" Subsonic Wind Tunnel Data, General Dynamics Convair. (April 2, 1963).

[3] "Six-degree-of-freedom flight-path study generalized computer program," McDonnell Aircraft Corp., Flight Dynamics Lab., St. Louis, Mo., Contract AF33(616)-6848, Wright Air Development Div. TR60-781 (May 1961).

[4] Buscis, G. W., "Effects of the jet exhaust on the second stage of the ATHENA missile," Atlantic Research Corp. Rept. 7920-07 (April 1963).

[5] Augustine, F. F., "Revision to nominal trajectories and associated stage impact dispersions for the ATHENA vehicle," Aerospace Corp. Memo A63-1742.2-3 (January 1963).